Available online at www.sciencedirect.com
SCIENCE DIRECT®

Journal of the European Ceramic Society 24 (2004) 811–819

www.elsevier.com/locate/jeurceramsoc

Recovered slate waste as raw material for manufacturing sintered structural tiles

M. Campos*, F. Velasco, M.A. Martínez, J.M. Torralba

Universidad Carlos III de Madrid, Avd. Universidad 30,E- 28911 Leganes, Spain

Received 8 January 2003; received in revised form 2 April 2003; accepted 13 April 2003

Abstract

Since roofing slate exploitations generate large quantities of slag from the quarry and mud from the cutting tools, special efforts are needed to avoid associated environmental hazards, such as floods and the unsightliness of slag-heaps. Recovering this mud and slag as raw material for manufacturing sintered structural parts could be a response to the demand. This study, which includes a characterisation of the material and an evaluation of the final properties, examines the raw material and its behaviour during compaction to determine whether it is suitable for processing by powder technology. A mineralogical characterisation by chemical analysis and X-ray diffraction, together with a thermal analysis, provided the data of the sintering process. The properties of the sintered samples were checked by: density, dimensional change, volume loss, mass decrement, three-point bending strength, water absorption and permeability, and wear behaviour trying to guarantee their behaviour.

Keywords: Ceramic powder technology; DTA-TG; Functional applications; X-ray diffraction; Wastes

1. Introduction

According to Bates and Jackson,[1] slate is a compact metamorphic stone formed as a result of the sedimentation of fine material deposits subjected to the action of high temperatures and pressures. Although the composition depends on area formation, varieties of slate are classified according to colour, and this in turn depends on the composition and the grain size of the chlorite, density, water absorption coefficient, bending strength, etc.[2] The mineralogical composition of slates includes: quartz, phyllosilicates (as chlorites and muscovite) and illite (micaceous mineral from clay). Smaller amounts of others minerals are often present: iron oxides and sulphides—unfavourable for final applications—and carbonates.

Given the planar structure of slate, it may be split into thin plates to be directly used directly for tiles,[3] so it is mainly an architectural element for roofing, flooring and paving.[4,5] Slate extraction, however, generates large volumes of waste, normally deposited as slag, which damage drainage system, and certainly modifies the environment with land filling. Gonzalez et al.[6] proposed methods of minimizing this waste, either by its re-utilization or by cutting by laser.[7–9] They classified the wastes according to size, and defined possible uses for material of grain size below that of the ASTM 200 sieve. The proposed uses included the manufacture of cement, refilling microholes in the production of rolled asphalt layer for road, insulator of walls by a foam structure, and as arid aggregates.

Environmental impact is not of course the only consideration; the health effects and alterations of dust inhalation by workers have also been signalled.[10]

This paper gives the results of a feasibility study of the recovery of waste mud and slag for use as a raw material for sintered structural parts manufactured by powder technology. Mud can be introduced directly into the processing route, whereas slag needs to be properly crushed and sieved.[11] The aim is to determine the compacting pressure and the sintering temperature that give the best properties, as well as the maximum particle size of slate waste, for good quality tiles.

* Corresponding author.
E-mail address: campos@ing.uc3m.es (M. Campos).

0955-2219/03/$ - see front matter © 2003 Elsevier Ltd. All rights reserved.
doi:10.1016/S0955-2219(03)00325-X

Table 1
Chemical composition of slate waste calculated from atomic absorption results

Oxides	Processing plant (mud)	Quarry (slag)
SiO_2	54.9–50.7	55.4–51.3
Al_2O_3	22.4–20.0	22.8–21.5
Fe_2O_3 + FeO	13.5–11.8	13.3–11.7
K_2O	6.0–5.7	7.1–6.4
Other oxides[a]	8.3–6.7	6.0–5.0
Ignition loss	7.8	3.6

[a] TiO_2, MnO, MgO, CaO, K_2O, Na_2O.

2. Experimental procedure

The waste was collected in Valdeorras area (Pizarras Las Arcas S.A. Spain), both in the quarry and in the processing plant. The quarry slag was milled to a particle size below 320 μm and then materials were classified depending on their particle size and origin.

The first stage of development in powder technology comprises materials characterization. In this case, this step was done through X-ray diffraction (with Cu anticathode) to determine mineralogical composition, as well as by chemical analysis (Table 1), and by SEM to examine the particle morphology and distribution. After mineralogical and chemical characterisation, we proceeded to measure the physical and mechanical properties of compacted and sintered specimens. In order to find the best properties balance, three kinds of powder were prepared as raw material using the different particle size distributions: A: $\phi_a < 200$ μm, B: $200 < \phi_b < 320$ μm and M: mud, with a narrow particle size distribution and close to 20 μm, previously dried for 2 h at 100 °C before its use, as recommended in Ref. 12.

To better understand sintering behaviour, the mud has been subjected to simultaneous thermal analysis (STA), which records simultaneously TG (thermogravimetric) and DTA (differential thermal analysis). In this case the tests have been run in air up to 1400 °C with a heating and cooling rate of 3 °C/min.

To find the best balance of properties, the samples have been uniaxially pressed in a floating die as rectangular specimens of 100×35 mm at three compacting pressures (30, 35 and 45 MPa) to obtain green compacts. These have been sintered at two temperatures, 1100 and 1150 °C, for 30 min in air. Dimensional change (as volume loss) has been measured in all sintered samples it, weight loss, density, bending strength and permeability were measured by the usual standards. Wear behaviour has been determined by a pin-on-disc test under extreme conditions that reveal the differences between all materials:

- Applied load: 5 N.
- Pin: 6 mm diameter alumina ball.
- Sliding speed: 0.35 m/s.
- Humidity: below < 30%

To ensure uniform conditions, all material surfaces have been ground to 180 μm. Wear has been studied by dimensional wear coefficient k.[13] To evaluate the effect of sliding distance once steady state had been achieved, pin-on-disc test was done up to 500, 1000 and 2000 m. The slate tiles were then compared with used sidewalk tile.

3. Results and discussion

3.1. Raw material characterization

Chemical analysis of slag and mud are shown in Table 1, where silica, alumina and iron oxides are the principal components. No important difference was found between batches from quarry or those from the processing plant. Pairing the results of X-ray (Fig. 1)

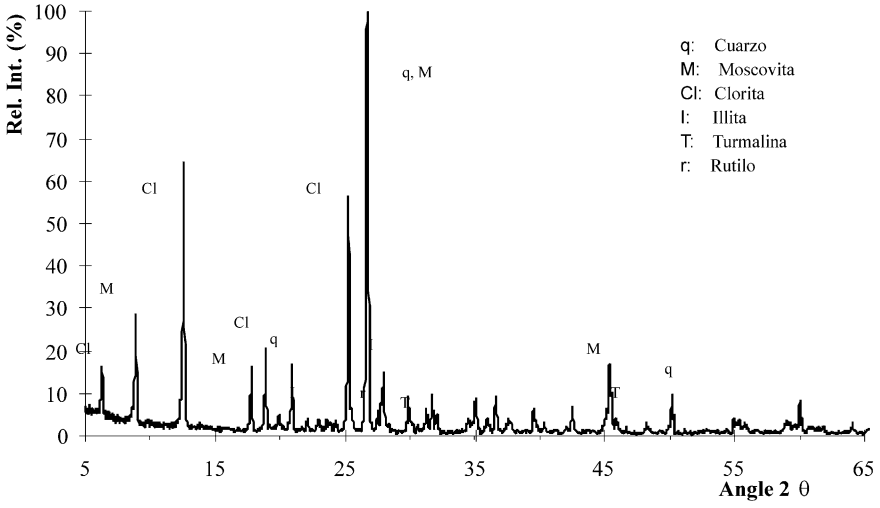

Fig. 1. Slate diffraction pattern.

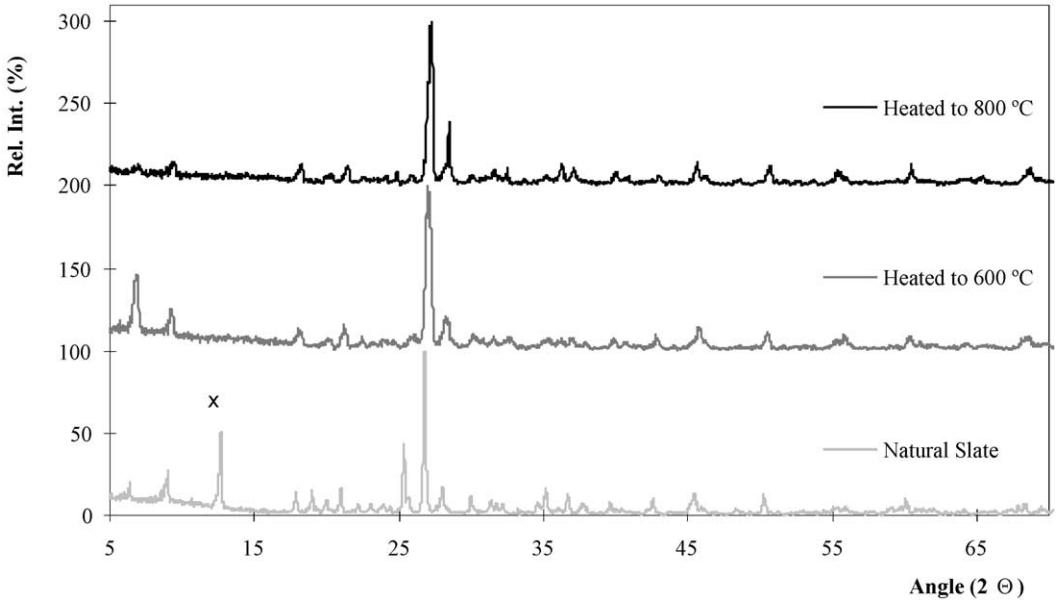

Fig. 2. XRD Heating test of slate waste (the third peak belonging to chlorite marked in the graphic was lost).

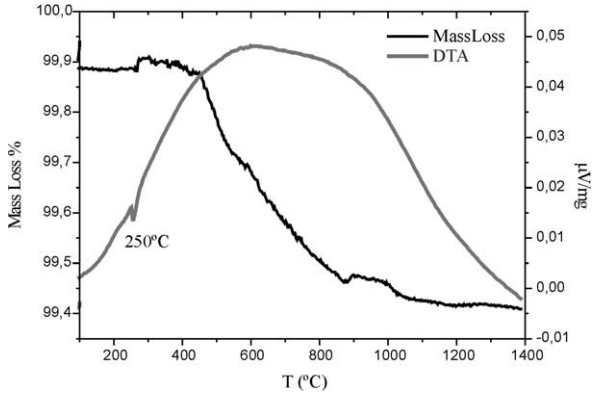

Fig. 3. STA measurements of slate.

with chemical analysis, the oxides that predominatein the slate are seen to be SiO_2 and Al_2O_3, because of the presence of clay minerals and quartz. The other oxides are of: *Fe* (from Chamosite and Tourmaline), *K* (appears in Muscovite and Illite), *Mg* (from Chlorite, either chamosite or clinochlore, Illite and Tourmaline), *Ti:* (like Rutile), *Na* (mainly from Tourmaline) and *Ca* (from Illite and Tourmaline). Diffraction also revealed the evolution of the different phases with the temperature (Fig. 2).

Two samples with $\phi < 200$ μm were heated up to 600 and 800 °C for 2 h. The effect of increasing temperature was reflected in chlorites that disappear if the slate is heated up to 600 °C. At 800 °C no other mineral disappears, but the relative intensity of the peaks

Fig. 4. Silicate. Typical flake morphology.

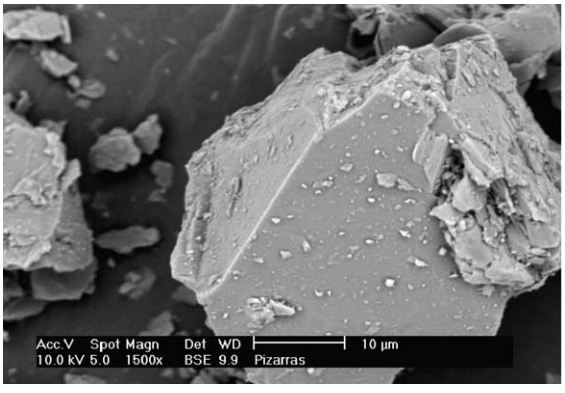

Fig. 5. Quartz-Prismatic shape. The same morphology was found for illite and rutile.

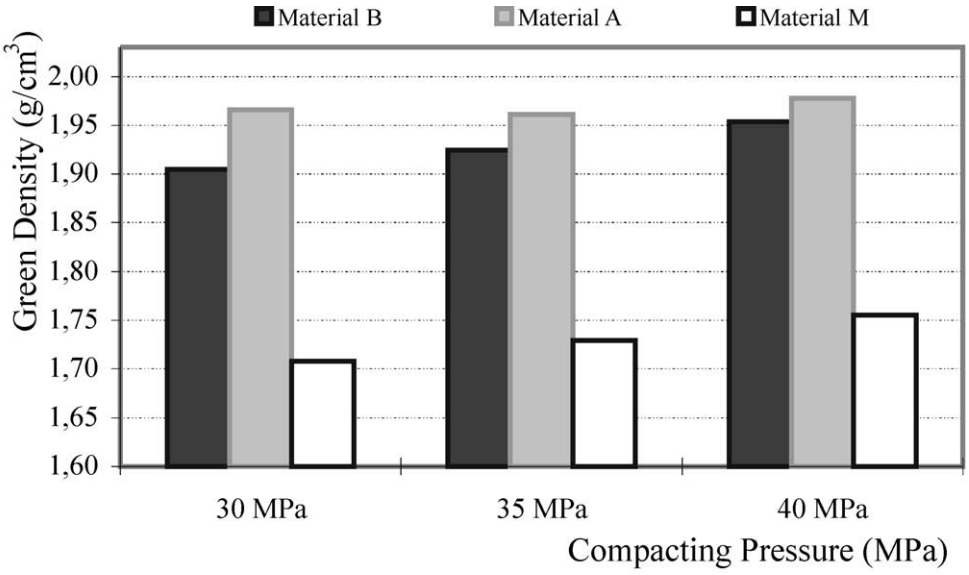

Fig. 6. Green densities of test samples compacted at 30, 35 and 40 MPaF.

decreases. No other structure of olivine group [a mineral silicate of iron and magnesium, principally (Mg, $Fe)_2SiO_4$] appeared, recrystallization would take place at higher temperatures (up to 900 °C) as vitreous phase.

STA analysis illustrated behaviour of the slate with temperature (Fig. 3). The first peak at around 250 °C can be attributed to water elimination (OH). Between 450 and 900 °C, TG traces show signs of decomposition from mineral net destruction and—according to X-ray patterns—to chlorite, either chamosite (Fe^{2+}, Mg, Fe^{3+}, Al) $(SiAl)_2O_5$ $(OH)_4$ or clinochlore $(Mg\ Al)_6(Si\ Al)_4O_{10}(OH)_8$ since muscovite and, in general, mica (except illite) are thermally inert[14,15]

SEM revealed the morphology of the particles of various minerals, either prismatic or as sheets with a flag and slab appearance. Silicates belong to sheet group (Fig. 4) whereas oxides appeared as prismatic (Fig. 5).

3.2. Compaction behaviour

Water was used as particle binder to give an adequate plasticity to fill the die before pressing. The green density was measured in samples with different particle distribution (Fig. 6). Materials B and M showed the lowest green densities because their incomplete particle size distribution. Material B had the largest particles sizes, in the range ∈ [200–320] μm, and M material only has the smallest. This small particle size of the mud hindered compaction and lowered green densities.

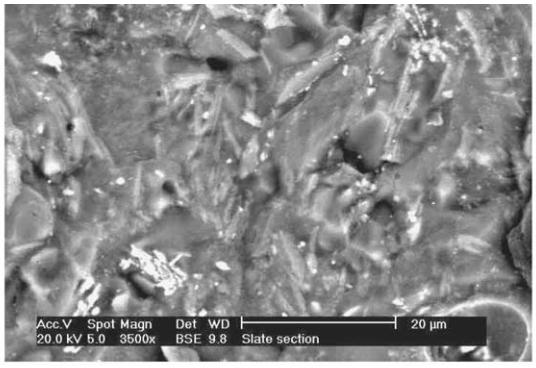

EDS microanalysis %wt	
SiO_2	81.07
Al_2O_3	9.75
Other oxides traces	9.18

Fig. 7. Weight loss of mud depending on sintering temperature vs. green density.

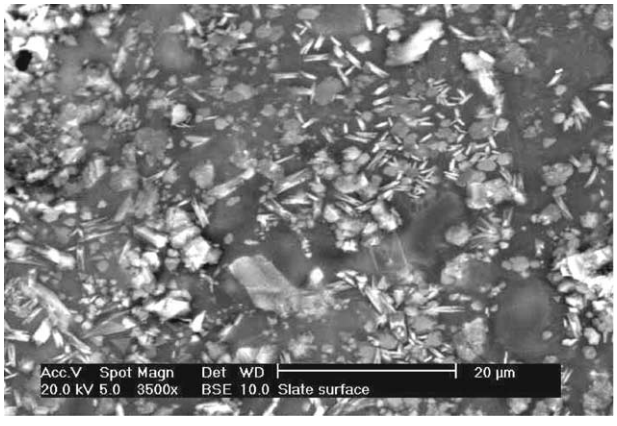

Fig. 8. Vitreous phase at surface.

At same compacting pressure, material A with a complete particle size distribution showed higher green density on account to the better rearrangement.

3.3. Sintering behaviour

After sintering, the weight loss was evaluated. Fig. 7 shows the results from samples manufactures with mud. With sintering at 1100 °C—the temperature at which conventional ceramic materials are fired—the weight loss of mud increases with the compacting pressure following green density behaviour. But when they are sintered at 1150 °C, the weight loss decreases with the higher pressure because of the formation of amorphous silica at this temperature (Fig. 8). It acts as a vitreous phase that fills the pores, and the lower porosity impedes the volatile losses.

The vitreous phase agglomerates the other minerals remaining in slate waste after the sintering process (Fig. 9).

Shrinkage indicates the degree of densification during sintering. Sample shrinkage increases as the particle size decreases, since the increase of particle necks assists diffusion and therefore, enhances sintered mechanisms. Given the presence the presence of amorphous silica on sintering at 1150 °C, the materials that chow the greatest dimensional changes are those manufactured from mud powder (Material M) (Fig. 10). The densification is influenced by particle size, compacting pressure and sintering temperature. The highest density is that of to

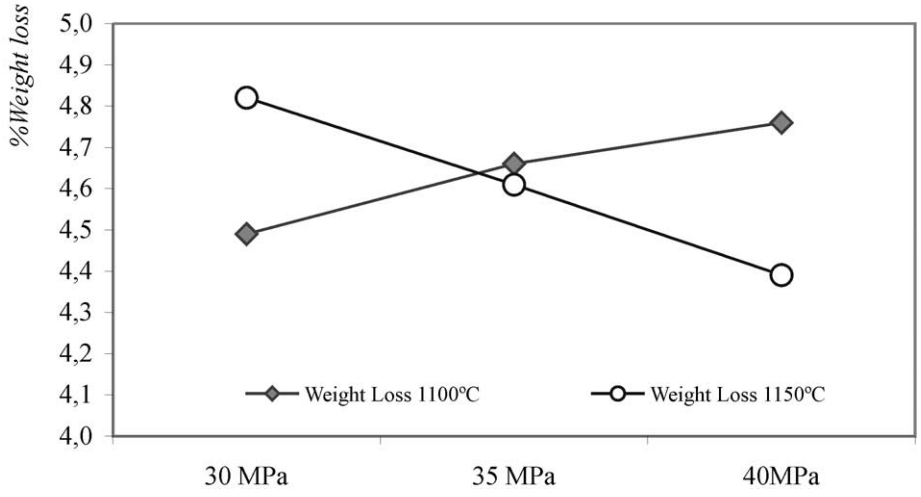

Fig. 9. Sintered surface of mud specimen examined by SEM.

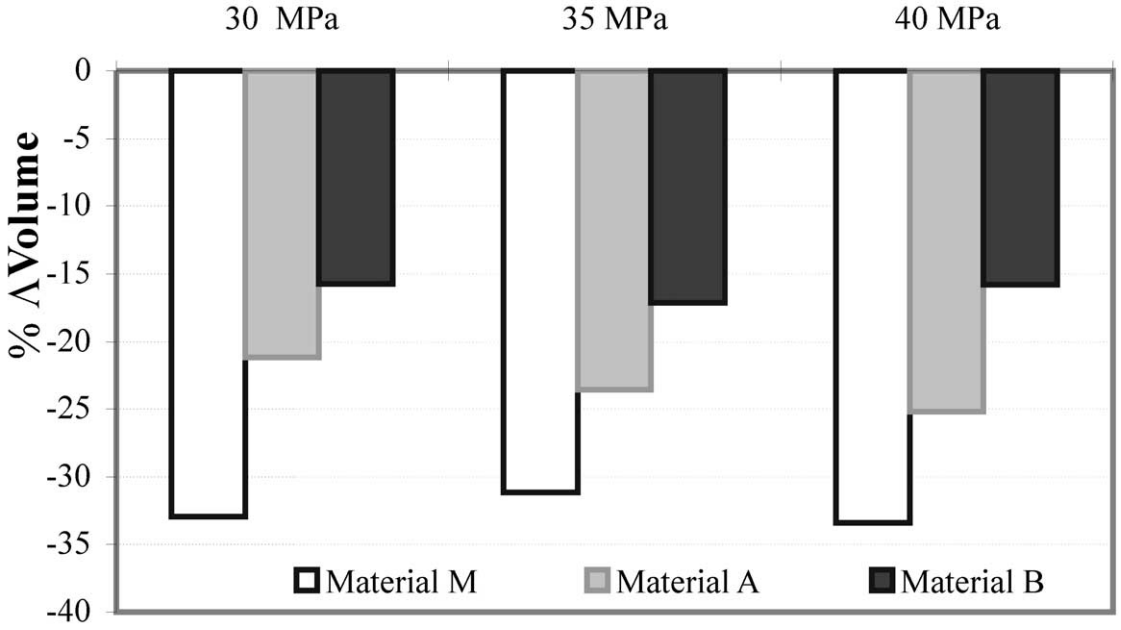

Fig. 10. Volume change in samples sintered at 1150 °C.

mud and the lowest that of material B with a particle size distribution between [200–320] due to the absence of smaller particle sizes. M with the lowest green density, reached the highest sintered density.

Following the process that was described in Ref. 16 the density and water absorption were measured in sintered test samples. (See Figs. 11 and 12). In samples sintered at 1100 °C, the density and water-absorbed values were in good agreement, giving an indication of incomplete sintering. Densities varied between 2 and 2.2 g/cm^3. The higher sintering temperature (Fig. 12) promoted the presence of a vitreous phase, allowing the sintering process to proceed by mass transfer from a high viscosity solid to a solid phase, which affects the microstructure, density and mechanical properties, reduces water absorption. The densities varied between 2.2 and 2.45 g/cm^3.

The bending strength is highly influenced by the sintering temperature (Fig. 13). Since the mechanisms of sintering are completely activated, the bending strength increases with the temperature. Sintering was found to be more effective in samples manufactured from mud, due to the higher specific surface of the particles and the consequent better densification. The compacting pressure is not the governing factor in this processing route if the samples have not been properly sintered.

The suitability of these materials for the manufacture of roof tiles was determined by permeability measurements. This test gives the time (t) that a drop of water takes to pass through the sample. Depending on this time, materials are classified as quality a, b, or the best c. The material is not suitable for the manufacture of roof tiles if the drop passes through in less than 2 h. Table 2 shows that all the materials sintered at 1150 °C

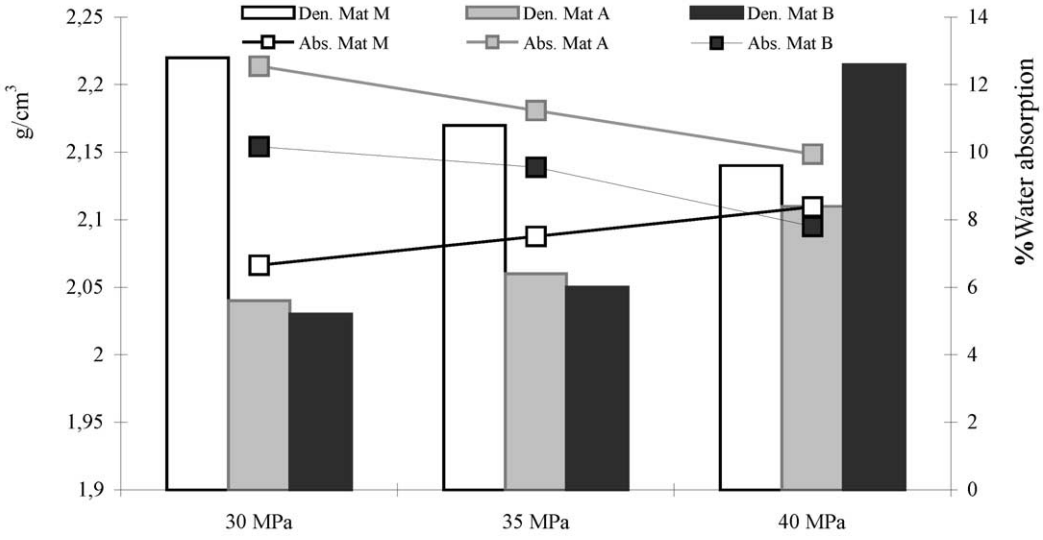

Fig. 11. Density and water absorption in samples sintered at 1100 °C.

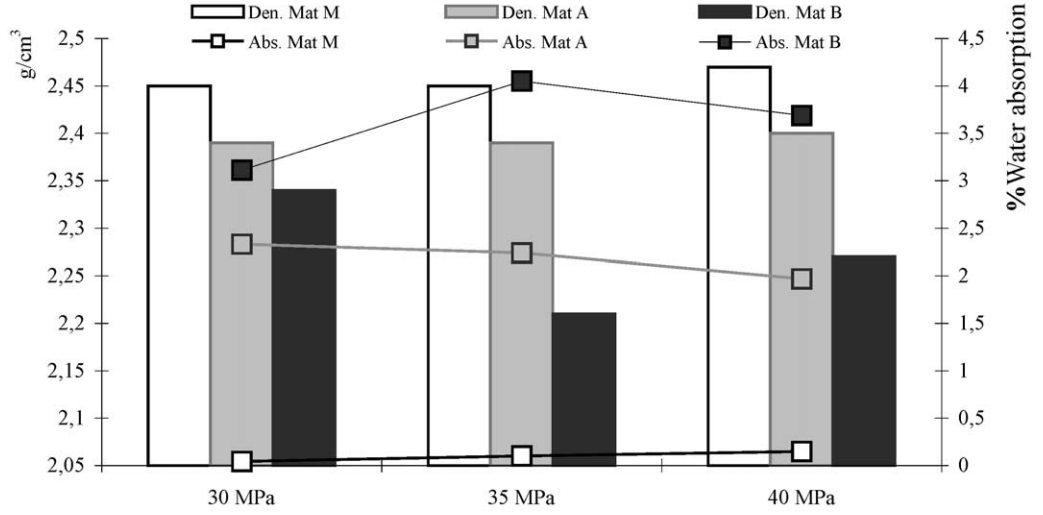

Fig. 12. Density and water absorption in samples sintered at 1150 °C.

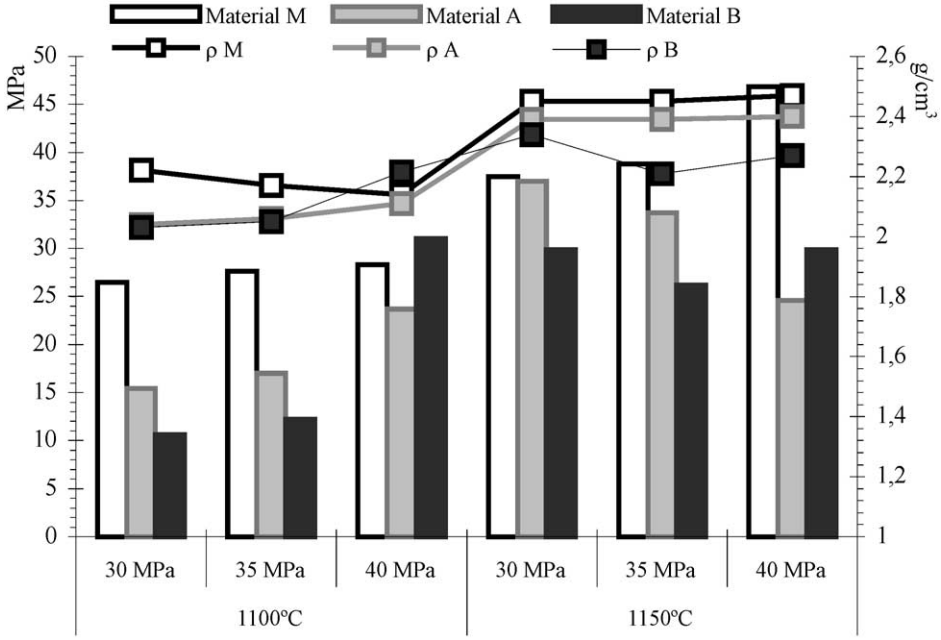

Fig. 13. Bending strength.

were found suitable for the manufacture of roof tiles. Those sintered at 1100 °C showed poor permeability properties, and even material A proved unsuitable, and of course material B.

3.4. Wear behaviour

In the course of the pin-on-disc test, abrasion is the main wear mechanism. The alumina pin showed no sign of wear and retained its shape and weight. The track formed on the surface of the slate samples was uniform, without lateral or internal cracks.

As a consequence of applied load, the tracks underwent vitrification so the dimensional wear coefficient (k) decreases as sliding distance increases (Table 3). After a sliding distance of 2000 m, k remains constant independently of particle size distribution a clear indication of track vitrification. Since wear is due mainly to abrasion, a higher particle size distribution reduces the k values, so material B showed the lowest wear, and the most favourable process was for material B and for low compacting pressure.

Comparison with a conventional sidewalk tile (Fig. 14) revealed the magnitude of wear coefficient. Tiles com-

Table 2
Permeability of sintered samples

Compacting pressure (MPa)	First drop time (h)	Remarks	
1150 °C			
A	30	> 24	Suitable CLASS c
	35	> 24	Suitable CLASS c
	40	> 24	Suitable CLASS c
B	30	> 24	Suitable CLASS c
	35	> 24	Suitable CLASS c
	40	> 24	Suitable CLASS c
M	30	> 24	Suitable CLASS c
	35	> 24	Suitable CLASS c
	40	> 24	Suitable CLASS c
1100 °C			
A	30	< 2	Not suitable
	35	< 2	
	40	< 2	
M	30	$12 < t < 24$	Suitable CLASS b
	35	> 24	Suitable CLASS c
	40	> 24	Suitable CLASS c

Table 3
Dimensional wear coefficient k (10^{-3} mm^3/Nm) vs. sliding distance regarding with compacting pressures on samples sintered at 1150 °C

Compacting Pressure MPa	Sliding distance (m)	Mat A	Mat B	Mat M
30	500	2.04	0.45	1.80
	1000	1.89	0.68	1.39
	2000	0.95	0.37	1.36
35	500	2.03	1.19	1.99
	1000	1.79	0.90	1.00
	2000	1.18	0.59	1.13
40	500	2.20	0.97	1.68
	1000	1.06	0.96	1.22
	2000	0.83	0.77	0.73

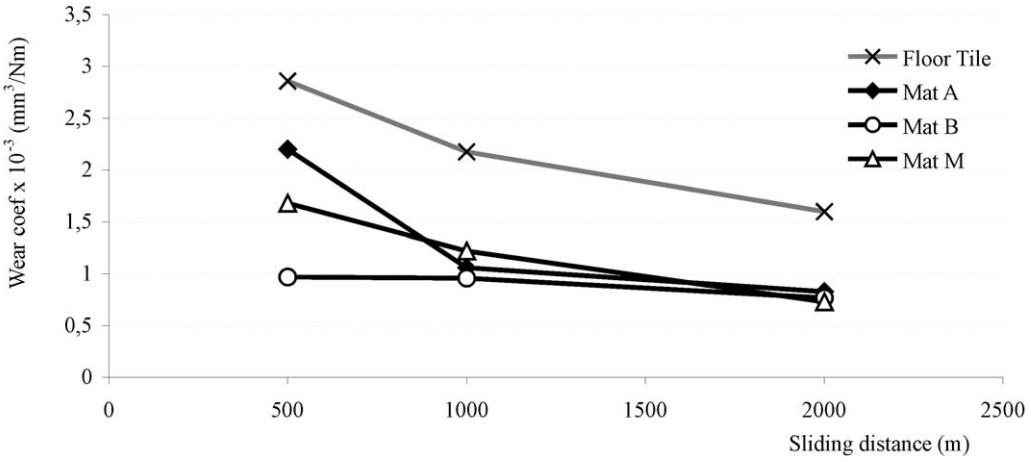

Fig. 14. Wear coefficient comparison.

pacted at 40 MPa and sintered at 1150 °C were found to be the best. The comparison showed that slate tiles are an appropriate material for floor tiles.

4. Conclusions

All the measurements showed that materials obtained from slate waste are suitable for use as the raw material for ceramic tiles since their properties are within the range of those of conventional ceramic tiles

- The characterisation of slate particles showed them to be an appropriate raw material for the production of tiles by powder techniques. For its correct incorporation, the mud must be atomised to fill the die in an automated process.
- Compaction pressure is not the governing factor in this processing route if samples have not been sintered properly. Amorphous silica formed by sintering at 1150 °C improves properties by assisting its diffusion.
- The wear measured as a dimensional wear coefficient decreases with the sliding distance as ma consequence of the glass vitrification promoted by the applied load.
- In comparison with that of conventional sidewalk tiles, the wear coefficient of slate tiles shown proved their suitability for this application.

Acknowledgements

The authors thank the European Union for the financial support through the Project CRAFT BRST CT95-0063, which aided the initial part of this work reported in Ref. 16.

References

1. Bates, R. L. and Jackson, J. A., *Glossary of Geology*, 3rd edn. Am. Geol. Inst, 1987.
2. Nieves Aguirre, G., *Natural Stones. Directory*. Roc Máquina, SA, Spain: Bilbao, 1997.
3. Bastida, F., La equistosidada primaria, una síntesis sobre sus características y desarrollo. *Oviedo University, technical Seminar*, 1981, **11**, 35–54.
4. García de los Ríos Cobo, J. I. and Báez Mezquita, J. M., *La pizarra en Castilla y León*. Ed. Junta de Castilla y León, 1997.
5. Menéndez Seigas, J. L., Arquitectura y tecnología de la colocación de pizarra en cubiertas. *Peymar Artes Gráficas, S. L. O Barco (Ourense)*, 1993, **Spain**, 18–20.
6. González, C., Taboada, J., Menéndez, A. and Álvarez, A. E., Geological risk in slag heaps of roofing slate in Spain. *Int. J. Surf. Mining, Reclamation and Environment*, 1997, **11**, 145–150.
7. Boutinguiza, M., Pou, J., Lusquiños, F., Quintero, F., Soto, R., Pérez-Amor, M., Watkins, K. and Steen, W. M., CO2 laser cutting of slate. *Optics and Lasers in Engineering*, 2002, **37**, 15–25.
8. Lusquiños, F., Pou, J., Soto, R. and Pérez-Amor, M., The drilling of slate tiles by a Nd: YAG laser. *J Laser Appl*, 1997, **9**, 211–214.
9. Larosi, M., Lusquiños, F., Pou, J., Soto, R. and Pérez-Amor, M., NdYAG laser cutting of slate. *Proceedings of ICALEO. Laser Mater. Process. LIA*, 1998, **85**, B–165-172.
10. Rego, G., Martínez, C., Quero, A., Blanco, T. P. and Borquea, J. M., The effects of dust inhalation in slate industry workers. *Medicina Clinica*, 2001, **116**(8), 290–291.
11. Basegio, Tania, Berutti, Felipe, Bernardes, Andréa and Pérez Bergmann, Carlos, Environmental and technical aspects of the utilisation of tannery sludge as a raw material for clay products. *C.P. J. Eur. Ceram. Soc.*, 2002, **22**(13), 2251–2259.
12. Cassano, E. and Drioli and, R., Molinari, Saving of water and chemicals in tanning industry by membrane processes. *Water. Res.*, 1999, **4**, 443–450.

13. Williams, J. A., *Engineering Tribology*. Oxford Science Publications, 1998.
14. Rodriguez, M. A., Rubio, F., Rubio, J., Liso, M. J. and Oteo, J. L., Caracterización estructural y comportamiento térmico de una muestra de pizarra empleada como material para la edificación. *Boletín Geológico y Minero*, 1995, **106–5**, 437–445.
15. Aleixandre, V., ATD de algunas arcillas y caolines españoles. *Anal. Edaf.*, 1949, **8**, 33–58.
16. Spanish Standard UNE 22-191-85.